JVI Journals.ASM.org

Interferon Response Factors 3 and 7 Protect against Chikungunya Virus Hemorrhagic Fever and Shock

Penny A. Rudd,[a,b] Jane Wilson,[a,c] Joy Gardner,[a] Thibaut Larcher,[d] Candice Babarit,[d] Thuy T. Le,[a] Itaru Anraku,[a] Yutaro Kumagai,[e] Yueh-Ming Loo,[f] Michael Gale, Jr.,[f] Shizuo Akira,[e] Alexander A. Khromykh,[b] and Andreas Suhrbier[a,b]

Queensland Institute of Medical Research, Brisbane, Queensland, Australia[a]; Australian Infectious Diseases Research Centre, School of Chemistry & Molecular Biosciences, University of Queensland, Brisbane, Queensland, Australia[b]; School of Medicine, University of Queensland, Brisbane, Queensland, Australia[c]; Institut National de Recherche Agronomique, Unité Mixte de Recherche 703, Ecole Nationale Vétérinaire, Nantes, France[d]; Laboratory of Host Defense, WPI Immunology Frontier Research Center, Osaka University, Osaka, Japan[e]; and Department of Immunology, University of Washington School of Medicine, Seattle, Washington, USA[f]

Chikungunya virus (CHIKV) infections can produce severe disease and mortality. Here we show that CHIKV infection of adult mice deficient in interferon response factors 3 and 7 (IRF3/7$^{-/-}$) is lethal. Mortality was associated with undetectable levels of alpha/beta interferon (IFN-α/β) in serum, ~50- and ~10-fold increases in levels of IFN-γ and tumor necrosis factor (TNF), respectively, increased virus replication, edema, vasculitis, hemorrhage, fever followed by hypothermia, oliguria, thrombocytopenia, and raised hematocrits. These features are consistent with hemorrhagic shock and were also evident in infected IFN-α/β receptor-deficient mice. *In situ* hybridization suggested CHIKV infection of endothelium, fibroblasts, skeletal muscle, mononuclear cells, chondrocytes, and keratinocytes in IRF3/7$^{-/-}$ mice; all but the latter two stained positive in wild-type mice. Vaccination protected IRF3/7$^{-/-}$ mice, suggesting that defective antibody responses were not responsible for mortality. IPS-1- and TRIF-dependent pathways were primarily responsible for IFN-α/β induction, with IRF7 being upregulated >100-fold in infected wild-type mice. These studies suggest that inadequate IFN-α/β responses following virus infection can be sufficient to induce hemorrhagic fever and shock, a finding with implications for understanding severe CHIKV disease and dengue hemorrhagic fever/dengue shock syndrome.

Chikungunya virus (CHIKV) is a mosquito-borne, single-stranded, positive-sense RNA virus (genus *Alphavirus*) that has caused sporadic outbreaks of predominantly rheumatic disease, primarily in Africa and Asia (57). CHIKV disease was often confused with dengue because of similarities in clinical presentation (5); however, this continues to be an issue only in the absence of appropriate serological and/or molecular diagnosis (2). The largest documented outbreak of CHIKV disease ever recorded occurred during 2004-2011, starting in Kenya, spreading across the Indian Ocean Islands to India and Southeast Asia, and reaching New Caledonia in 2011. Over 260,000 cases (about one-third of the population) were reported in Reunion Island (France), and an estimated 1.4 to 6.5 million cases occurred in India. The first autochthonous CHIKV infections in Europe were seen in Italy in 2007 and France in 2010. Due to international travel, imported cases were reported in nearly 40 countries, including European countries, Japan, and the United States. Although *Aedes aegypti* is the classical vector for CHIKV, the recent outbreak was associated with the emergence of a new clade of CHIKVs, which were efficiently transmitted by *Aedes albopictus* mosquitoes, a vector that has seen a dramatic global expansion in its geographic distribution. The recent CHIKV outbreak was also associated with severe disease manifestations and some mortality. At present, no licensed vaccine or particularly effective drug is available for human use for any alphavirus, although analgesics and nonsteroidal anti-inflammatory drugs can provide relief from rheumatic symptoms (53, 57).

IFN-α/β and antiviral antibodies have been shown to be important for protection against infection, disease, and/or mortality caused by CHIKV and other alphaviruses (15, 53, 57). CHIKV infection of IFN-α/β receptor-deficient mice results in death, with IFN-α/β receptor expression on nonhematopoietic cells being required for protection (51). In addition, CHIKV infection does not appear to stimulate significant IFN-α/β production in hematopoietic cells, with IFN-α/β being largely produced by infected nonhematopoietic cells (51). At least three host sensor pathways have been implicated in the production of IFN-α/β during CHIKV infection; these involve (i) the RIG-I-like receptors, retinoic acid-inducible gene I (RIG-I), melanoma differentiation-associated gene 5 (Mda5), and signaling via interferon-β promoter stimulator 1 (IPS-1; also known as MAVS, VISA, and Cardif); (ii) Toll-like receptor 3 (TLR3) signaling via TIR domain-containing adaptor-inducing interferon-β (TRIF); and (iii) Toll-like receptor 7 (TLR7) signaling via myeloid differentiation primary response gene 88 (MyD88) (51, 53, 66).

Downstream of RIG-I/Mda5/IPS-1, TLR3/TRIF, and TLR7/MyD88 lie interferon regulatory factor 3 (IRF3) and interferon regulatory factor 7 (IRF7), two key transcription factors involved in the induction of IFN-α/β (53), with IRF7 upregulation being important for induction of IFN-αs and the positive feedback that produces robust IFN-α/β responses (33, 48, 49). (In myeloid cells, IRF3/7-independent IFN-α/β production has also been observed [10].) The central role of IRF3 and/or IRF7 has been illustrated for a number of viruses by the use of IRF7$^{-/-}$ and/or IRF3$^{-/-}$ mice. For instance, IRF7$^{-/-}$ and IRF3$^{-/-}$ mice infected with encepha-

Received 18 April 2012 **Accepted** 25 June 2012
Published ahead of print 3 July 2012
Address correspondence to Andreas Suhrbier, andreasS@qimr.edu.au.
Supplemental material for this article may be found at http://jvi.asm.org/.

doi:10.1128/JVI.00956-12

lomyocarditis virus showed significantly higher levels of mortality than wild-type (WT) mice (22). In contrast, infection with herpes simplex virus infection was lethal in IRF7$^{-/-}$ but not IRF3$^{-/-}$ mice (22). Increased mortality was also seen after infection of IRF7$^{-/-}$ or IRF3$^{-/-}$ mice with the virulent West Nile virus strain (NY99), whereas infection with the naturally attenuated West Nile strain (Kunjin) was universally lethal only in IRF3/7$^{-/-}$ double-knockout mice (9). IRF7 has been shown to be important for optimum production of IFN-α/β in murine embryonic fibroblasts (MEFs) after infection with a number of viruses (22) and is critical for IFN-α/β production by plasmacytoid dendritic cells (12). IRF3 has been shown to be important for optimum IFN-α/β production by nonhematopoietic and hematopoietic cells in response to certain virus infections (22), and IRF3-dependent apoptotic signaling can also contribute significantly to the host's protection from viral infection (4).

We recently developed an adult WT mouse model of CHIKV infection and rheumatic disease (15). Given the importance of IFN-α/β in protection against CHIKV infection (53) and the ability of CHIKV to inhibit IFN-α/β receptor signaling (14), we used this model to determine the relative importance of IRF3 and IRF7 in CHIKV infection and disease using IRF3$^{-/-}$, IRF7$^{-/-}$, and IRF3/7$^{-/-}$ mice. Infection in IRF3/7$^{-/-}$ mice was lethal, and interestingly, death was associated with hemorrhagic shock.

MATERIALS AND METHODS

Mice. IRF3$^{-/-}$ and IRF7$^{-/-}$ mice were generated by T. Taniguchi (University of Tokyo) (22, 49). These mice and IRF3/7$^{-/-}$ mice (10) were provided by M. S. Diamond (Washington University School of Medicine, St. Louis, MO). IPS$^{-/-}$ knockout mice on a C57BL/6 background were created using conventional methods (25) (see File S1 in the supplemental material). TRIF$^{-/-}$ and MyD88$^{-/-}$ mice have been described previously (68). All mice were on a C57BL/6 background. WT mice were purchased from Animal Resources Centre (Canning Vale, Western Australia, Australia).

Mouse infection and monitoring. Mice (6 to 12 weeks old) were inoculated with CHIKV (LR2006-OPY1), and virus titers and foot swelling were determined as described previously (15). Mice were inoculated with CHIKV (4 $\log_{10}$ 50% cell culture infective doses [$CCID_{50}$] in 40 μl RPMI 1640 supplemented with 2% fetal calf serum) by shallow subcutaneous (s.c.) injection into the top, toward the lateral side, of each hind foot in the metatarsal region, injecting toward the ankle. Arthritis (foot swelling) was monitored by measuring the height and width of the metatarsal area of the hind feet using digital calipers and is presented as a group average of the percentage increase in foot height times width for each foot compared with the same foot on day 0. No mycoplasma or endotoxin contamination was detected in the virus preparations by sensitive bioassays (23, 28). Animal work was conducted in accordance with good animal practice (NHMRC, Australia) and was approved by the Queensland Institute of Medical Research (QIMR) animal ethics committee.

Clinical measurements. Body temperature was measured using a digital thermometer (Digitech, Rydalmere, Australia) and a 2-mm thermocouple bead probe, which was lightly pressed for ~30 s into the pit of the rear leg of the restrained mouse with the leg folded over the probe. Urine output following urination induced by grasping the scruff was measured by collecting and weighing the urine produced within ~1 min of the mouse's being restrained. Blood platelet counts were determined using a hemocytometer and heparinized blood diluted 1/20 in phosphate-buffered 1% ammonium oxalate solution. Hematocrits were measured using standard hematocrit tubes (Becton Dickinson, North Ryde, New South Wales, Australia) and were expressed as the percent difference from control uninfected mice.

Cytokine and chemokine analyses. Serum cytokine and chemokine protein levels were analyzed by using the BD cytokine bead array bioanalyzer system (Becton, Dickinson, Franklin Lakes, NJ) according to the manufacturer's instructions. Bioactive IFN-α/β was measured by a cytopathic effect inhibition bioassay using Semliki Forest virus infection of L-929 cells as described previously (15).

Histology. Tissues were fixed in 10% neutral buffered formalin, feet were decalcified (15% EDTA in 0.1% phosphate buffer over 10 days), tissue was embedded in paraffin wax, and 6-μm-thick sections were cut and stained with hematoxylin-eosin. Slides were scanned using an Aperio Scan Scope XT digital slide scanner (Aperio, Vista, CA).

***In situ* hybridization.** A 450-bp digoxigenin-labeled CHIKV probe sequence (GenBank no. DQ443544.2; nucleotides 7371 to 7818) was hybridized to paraffin sections and detected with antidigoxigenin antibody conjugated with alkaline phosphatase. The corresponding region of RRV was used as a negative control. For details, see File S1 in the supplemental material.

Real time quantitative RT-PCR. RT-PCR was performed essentially as described previously (15). For details, see File S1 in the supplemental material.

Infection of MEFs. IRF3$^{-/-}$, IRF7$^{-/-}$, and IRF3/7$^{-/-}$ MEFs were seeded (2×10^5 per well) in 12 well plates, treated with the indicated amount of recombinant mouse IFN-α (Hycult Biotech, Uden, The Netherlands) overnight, and then infected with CHIKV (multiplicity of infection [MOI] = 0.1) for 2 h. The cells were washed and cultured, and supernatants were assayed for virus titers 24 h later.

Statistics. Analysis was performed using IBM SPSS statistics (version 19). The *t* test was used if the difference in the variances was <4, skewness was <−2, and kurtosis was <2; otherwise, the nonparametric Mann-Whitney U test was used. For survival analysis, the log rank statistic was used.

RESULTS

Chikungunya virus infection of IRF3$^{-/-}$, IRF7$^{-/-}$, and IRF3/7$^{-/-}$ mice. To determine the requirement for IRF3 and IRF7 for survival of CHIKV infection, IRF3$^{-/-}$, IRF7$^{-/-}$, and IRF3/7$^{-/-}$ mice were infected with a Reunion Island isolate of CHIKV (15). All IRF3/7$^{-/-}$ mice died between days 4 and 6 postinfection, whereas all IRF3$^{-/-}$, IRF7$^{-/-}$, and WT mice survived (Fig. 1A). Mortality in the IRF3/7$^{-/-}$ mice was associated with a significant increase in viremia, which was clearly evident from day 3 onwards and was ~4 logs higher than that seen in WT mice on day 5 (Fig. 1B). The viremia in IRF7$^{-/-}$ mice was ~1 log higher than that seen in WT mice on days 3 and 4 postinfection (Fig. 1B), but this approached significance only on day 3 ($P = 0.053$, Mann-Whitney U test). The viremia in IRF3$^{-/-}$ mice was not significantly different from that seen in WT mice (Fig. 1B). Viral titers in several organs were also substantially higher in IRF3/7$^{-/-}$ mice, often 6 to 8 logs higher, than those seen in WT mice (Fig. 1C). Although virus was found in brain (Fig. 1C), no overt neurological symptoms (altered gait, paralysis) were evident (data not shown). Viral titers in the feet were significantly higher (~3 logs, $P = 0.01$) in IRF3/7$^{-/-}$ mice than WT mice on day 6 (Fig. 1D). These experiments clearly show that either IRF3 or IRF7 is required for survival following CHIKV infection, with IRF3/7$^{-/-}$ mice showing significantly increased viremia, tissue titers, and disease as well as mortality occurring within several days of infection. Infection with an Asian isolate of CHIKV (15) was also lethal in IRF3/7$^{-/-}$ mice (data not shown).

Foot swelling after CHIKV infection. We have previously shown that WT mice produce a measurable foot swelling and arthritis on day 6 or 7 following CHIKV inoculation into feet (15). Similar infection of IRF3$^{-/-}$, IRF7$^{-/-}$, and IRF3/7$^{-/-}$ mice also

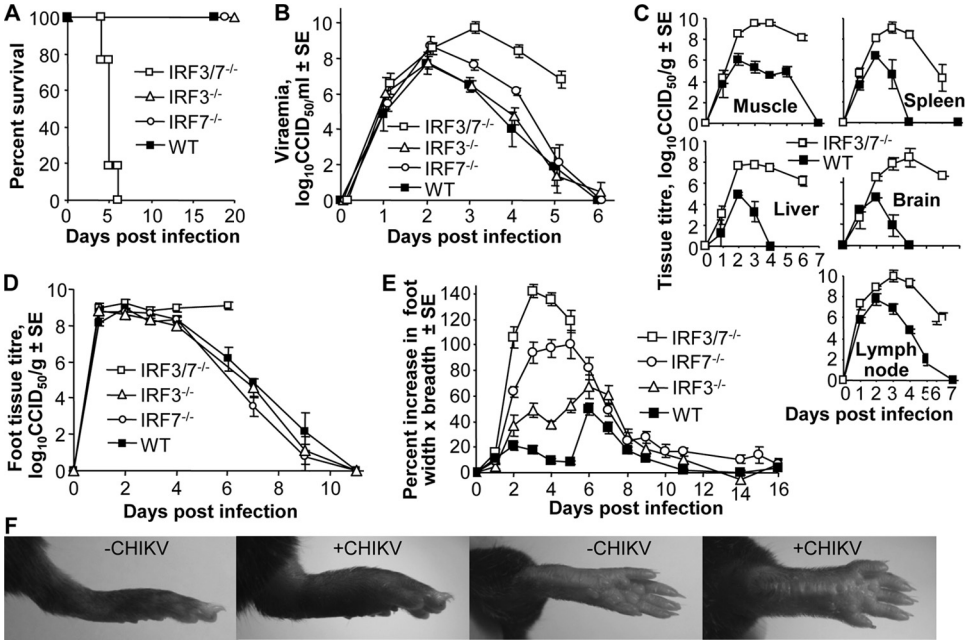

FIG 1 CHIKV infection in WT, IRF3$^{-/-}$, IRF7$^{-/-}$, and IRF3/7$^{-/-}$ mice. Mice (6 to 8 weeks old) were infected with CHIKV. (A) Mice were monitored daily, and a death event was recorded when an animal died or when animal welfare considerations required euthanasia (n = 12 to 20 per group; data are derived from three or four independent experiments). (B) Peripheral blood viremia (n = 7 to 12 per group; data are derived from three or four independent experiments). Differences between WT and IRF3/7$^{-/-}$ mice on days 3, 4, and 5 were significant ($P < 0.001$, $P = 0.004$, and $P = 0.014$, respectively; Mann-Whitney U test). (C) Tissue virus titers (n = 3 or 4 per group). Differences between WT and IRF3/7$^{-/-}$ mice were significant on days 3 and 4 (except for spleen on day 4) ($P < 0.05$; Mann-Whitney U test). (D) Virus titers in feet (n = 3 to 5 per group). Differences between WT and IRF3/7$^{-/-}$ mice reached significance on day 6 ($P = 0.01$, Mann-Whiney U test). (E) Percentage increase in foot swelling compared with day 0 (n = 30 feet per group, except for IRF3/7$^{-/-}$ day 6, where n = 6 feet). (Data are derived from three or four independent experiments.) (F) Photographs of feet from IRF3/7$^{-/-}$ mice before CHIKV infection (-CHIKV) and on day 4 postinfection (+CHIKV).

resulted in foot swelling, but swelling occurred much earlier (day 2 to 4) and was slightly more pronounced in IRF3$^{-/-}$ mice, substantially more pronounced in IRF7$^{-/-}$ mice, and even more pronounced in IRF3/7$^{-/-}$ mice (Fig. 1E and F).

Injection of heat-inactivated CHIKV (60°C for 30 min) into IRF3/7$^{-/-}$ or WT mice did not result in any significant swelling (data not shown). Although subcutaneous (s.c.) (base of tail) inoculation of CHIKV did not result in foot swelling in WT mice (15), this route of infection did result in some foot swelling in IRF3/7$^{-/-}$ mice (data not shown). Mortality in IRF3/7$^{-/-}$ mice was unchanged when virus was inoculated s.c. (data not shown).

Loss of IFN-α/β and elevated IFN-γ, monocyte chemoattractant protein-1 (MCP-1), interleukin 6 (IL-6), and tumor necrosis factor (TNF) in CHIKV-infected IRF3/7$^{-/-}$ mice. High levels of serum IFN-α/β (as measured by bioassay) were detected in WT mice after CHIKV infection (Fig. 2A), as reported previously (15). IRF3$^{-/-}$ mice showed serum IFN-α/β levels comparable to those seen in WT mice. However, only low levels of serum IFN-α/β were detected in IRF7$^{-/-}$ mice on day 2, and serum IFN-α/β was below detection in IRF3/7$^{-/-}$ mice (Fig. 2A). Real-time quantitative RT-PCR of feet on day 2 postinfection paralleled these findings, with the following rankings: for IFN-α mRNA levels, WT > IRF3$^{-/-}$ > IRF7$^{-/-}$ > IRF3/7$^{-/-}$ mice; for IFN-β mRNA levels, WT > IRF3$^{-/-}$ = IRF7$^{-/-}$ > IRF3/7$^{-/-}$ mice; for IFN-β mRNA, only low levels induced in IRF3/7$^{-/-}$ mice (Fig. 2B).

These observations suggest IRF7 is the main transcription factor involved in IFN-α/β production after CHIKV infection, an observation also reported for other viral infections (9, 22). The small amount of IFN-α/β seen in IRF7$^{-/-}$ mice appeared to be sufficient to contain the viremia (Fig. 1B) and prevent mortality (Fig. 1A), perhaps consistent with the high sensitivity of alphaviruses (35), including CHIKV, to IFN-α/β (55) (see Fig. 6).

The serum levels of inflammatory cytokines and chemokines were also measured in CHIKV-infected mice. IRF3/7$^{-/-}$ mice showed significantly elevated levels of IFN-γ, monocyte chemoattractant protein-1 (MCP-1, also known as CCL2), interleukin-6 (IL-6) (both peaking on day 2), and tumor necrosis factor (TNF) (elevated from day 2 to 6) compared with WT mice (Fig. 2A). On day 2 postinfection, serum from IRF3/7$^{-/-}$ mice contained >50-fold more IFN-γ and ~10-fold more MCP-1, IL-6, and TNF than that from WT mice (Fig. 2A). In IRF3$^{-/-}$ and IRF7$^{-/-}$ mice, the levels of these mediators were not significantly different from those in WT mice (Fig. 2A). Serum levels of IL-12 and IL-10 were not significantly changed, and IL-1β was not detected in any mouse strain (data not shown). The absence of detectable serum IFN-α/β in IRF3/7$^{-/-}$ mice thus appeared to correlate with very high levels of IFN-γ and high levels of other inflammatory mediators.

Mortality in IRF3/7$^{-/-}$ mice was associated with severe edema and hemorrhage. To gain insights into the mechanisms responsible for mortality in IRF3/7$^{-/-}$ mice, histological analysis of a number of tissues was undertaken on day 5 postinfection. Foot swelling was associated with severe generalized edema and multifocal severe hemorrhage, with the most severe lesions being observed deep in the dermis and subcutaneous tissues (Fig. 3A to

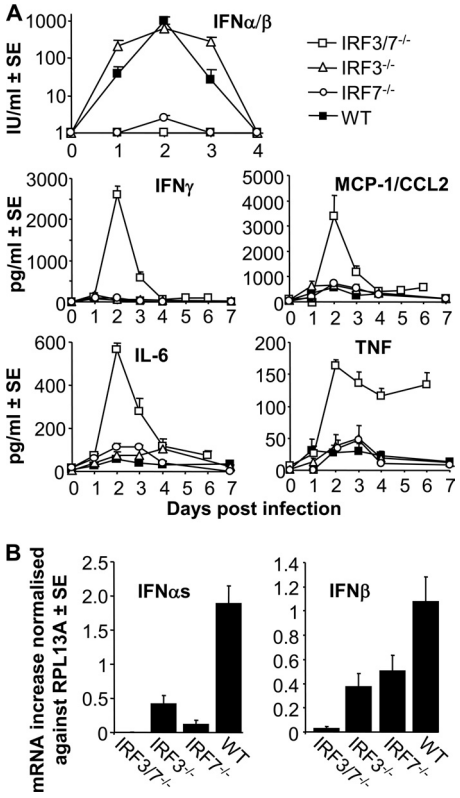

FIG 2 Cytokine and chemokine levels in the peripheral blood of CHIKV-infected mice. (A) WT, IRF3$^{-/-}$, IRF7$^{-/-}$, and IRF3/7$^{-/-}$ mice were infected with CHIKV, and peripheral blood samples were taken at the indicated times and assayed for the levels of the indicated cytokine or chemokine. The detection limit for the IFN-α/β bioassay was ~1 IU/ml. The levels in IRF3/7$^{-/-}$ mice were significantly different from those in WT mice on days 2 and 3 for all cytokines and chemokines, on day 1 for IFN-α/β, and on day 4 for TNF ($P < 0.034$, Mann-Whitney U test). Day 2 IFN-α/β levels were also significantly higher in IRF7$^{-/-}$ mice than in IRF3/7$^{-/-}$ mice ($P < 0.008$, Mann-Whitney U test) ($n = 4$ to 6 per group). (B) Quantitative real-time RT-PCR for IFN-αs and IFN-β mRNAs in feet on day 2 postinfection. Data were normalized to RPL13A (housekeeping gene) (15), and values for uninfected feet were subtracted ($n = 6$ to 8 per group). All differences were significant ($P < 0.03$) except that for IFN-β in IRF3$^{-/-}$ and IRF7$^{-/-}$ mice.

C). (Skin and subcutaneous tissue from uninfected IRF3/7$^{-/-}$ mice are shown in Fig. 3D.) Some hemorrhage was also evident in IRF7$^{-/-}$ mice (data not shown) but was not seen in IRF3$^{-/-}$ mice (data not shown) or in WT mice on day 5 postinfection (see File S2A and B in the supplemental material) or day 7 postinfection (15). Edema was marked in IRF7$^{-/-}$ mice but less severe than in IRF3/7$^{-/-}$ mice (data not shown). Edema was also present in IRF3$^{-/-}$ mice (data not shown) and WT mice on day 5 postinfection (see File S2A in the supplemental material) and day 7 postinfection (15).

IRF3/7$^{-/-}$ mice showed multifocal marked vasculitis characterized by fibrinoid necrosis of the vascular wall, with karyorrhexis of neutrophil nuclei, indicative of intramural leukocytoclasis (degenerate leukocytes inside the vascular wall), and perivascular fibrin exudation and extravasated red blood cells (Fig. 3C). Such lesions were mild or absent in WT mice on day 5 postinfection (see File S2C in the supplemental material) and day 7 postinfection (15). The mortality seen in CHIKV-infected IRF3/7$^{-/-}$ mice (Fig. 1A) thus appeared to be associated with severe edema, hemorrhage, and necrotizing vasculitis.

Scattered foci of marked skin necrosis with bulla formation were seen in the epidermis of IRF3/7$^{-/-}$ mice (Fig. 3E), with such lesions being rare or mild in IRF7$^{-/-}$ mice and not observed in IRF3$^{-/-}$ mice (data not shown) or WT mice (see File S2E in the supplemental material). (Epidermis from uninfected IRF3/7$^{-/-}$ mice is shown in Fig. 3F.) Exudative arthritis was evident, with inflammatory cells and fibrin present in joint synovia of IRF3/7$^{-/-}$ mice (Fig. 3G). Such lesions were not observed in IRF3$^{-/-}$ mice (data not shown) or WT mice on day 5 postinfection (see File S2D in the supplemental material) but are present in WT mice day 7 postinfection (15). Joint tissue from uninfected IRF3/7$^{-/-}$ mice is shown in Fig. 3H. Liver, spleen, muscle, lymph nodes, kidney, lung, intestine, and brain from IRF3/7$^{-/-}$ mice at 5 days postinfection were also examined. Apart from some lung consolidation, minimal leukocytic perivascular cuffs and slight pericapillary edema in the brain, and mild edema (see below) and mild focal hemorrhage in muscle tissues, no other significant lesions were seen (data not shown).

Paucity of cellular infiltrates and more endomysial edema in CHIKV-infected IRF3/7$^{-/-}$ mice. Only minimal cellular infiltrates were apparent in the swollen feet of IRF3/7$^{-/-}$ mice (Fig. 3A to C). This was evident in skeletal muscle of IRF3/7$^{-/-}$ mice (compare muscle from uninfected mice [Fig. 3I] with that from infected [Fig. 3J] mice) and contrasted with the abundant infiltrates seen in IRF7$^{-/-}$ (Fig. 3K), IRF3$^{-/-}$ (Fig. 3L), and WT mice on day 5 postinfection (see File S2F and G in the supplemental material) and day 7 postinfection (15). Muscle fiber necrosis was also evident in the latter three mice (Fig. 3K and L) (see File S2F in the supplemental material) (15) and is likely due to infiltrating macrophages (32).

Muscle tissue from CHIKV-infected IRF3/7$^{-/-}$ mice showed the occasional fragmented myocyte (Fig. 3J, arrow) and substantial endomysial edema (increased fluid between myocytes) (compare Fig. 3I and J), which was less severe in IRF7$^{-/-}$ mice (Fig. 3K) and not apparent in muscle from IRF3$^{-/-}$ mice (Fig. 3L) or WT mice (see File S2F and G in the supplemental material) (15).

Tissue localization of virus replication by *in situ* hybridization. The cells infected by CHIKV in adult WT animals have not been extensively characterized, although infection of monocytes/macrophages (21, 27), muscle satellite cells (40), and fibroblasts (53) has been observed in primates. *In situ* hybridization of WT feet on day 3 postinfection illustrated that CHIKV RNA could be detected in the cytoplasm of the following; (i) cells lining blood vessels, with morphology and location consistent with endothelial cells (Fig. 4A), (ii) skeletal muscle cells (Fig. 4B), (iii) rare cells in the dermis with morphology consistent with fibroblasts and macrophages (Fig. 4C), (iv) cells in the synovial membrane (Fig. 4D), and (v) cells of the periosteum (Fig. 4E). In IRF3/7$^{-/-}$ mice at 3 days postinfection, cells lining blood vessels and muscle fibers were also stained (Fig. 4F and G). Positive cells in the dermis were also found (most with fibroblastic and monocytic morphology) but were considerably more numerous in IRF3/7$^{-/-}$ mice (Fig. 4H). Some adnexal sebaceous glands also stained positive in the dermis (Fig. 4H, inset). A large number of positively staining cells (with location and morphology consistent with chondrocytes) were also seen in the articular cartilage of IRF3/7$^{-/-}$ mice (Fig. 4I), but such staining was not evident in WT mice (data not

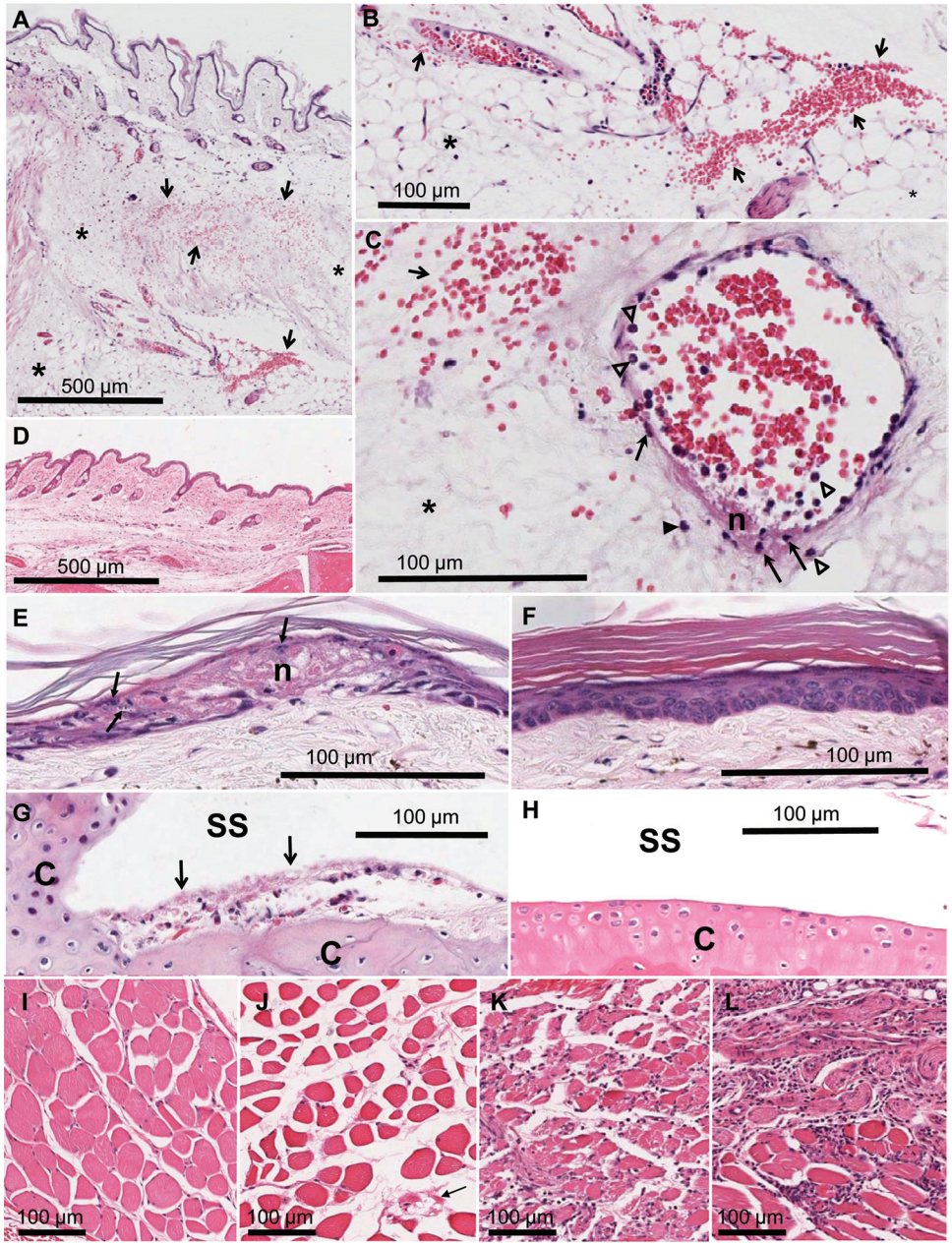

FIG 3 Histology of IRF3/7$^{-/-}$ mice after CHIKV infection. (A) Subcutaneous foot tissue 5 days after infection with CHIKV showing severe generalized edema (asterisks) and severe multifocal hemorrhage (arrows). (B) Enlargement of bottom of panel A showing edema (asterisk) and hemorrhage (arrows). (C) Vasculitis on day 5 characterized by vascular wall fibrinoid necrosis (n) and intramural degenerating leukocytes (arrows). Some neutrophils (white arrowheads) and mononuclear cells (black arrowheads) are present; an enlarged image is shown in File S5 in the supplemental material. (D) Subcutaneous foot tissue of an uninfected IRF3/7$^{-/-}$ mouse. (E) Focal skin necrosis (n) 5 days after infection of IRF3/7$^{-/-}$ mice with CHIKV. Keratinocytes undergoing ballooning degeneration, with pale cytoplasm and karyorrhectic nuclei (arrows), are evident. (F) Skin of uninfected IRF3/7$^{-/-}$ mice. (G) Exudative arthritis evident in the joints of an IRF3/7$^{-/-}$ mouse 5 days postinfection with CHIKV. Inflammatory cells and fibrin are present (arrows) in the synovial space (SS). Articular cartilage (C) is indicated. (H) Articular cartilage from an uninfected IRF3/7$^{-/-}$ mouse. Labels are as in panel G. (I) Skeletal muscle of an uninfected IRF3/7$^{-/-}$ mouse. (J) Skeletal muscle of an IRF3/7$^{-/-}$ mouse on day 5 postinfection. (K) Skeletal muscle of an IRF7$^{-/-}$ mouse on day 5 postinfection. (L) Skeletal muscle of an IRF3$^{-/-}$ mouse on day 5 postinfection.

shown). Positive cells were not detected in the synovial membranes of IRF3/7$^{-/-}$ mice (data not shown).

In WT mice at day 5.5, cells lining the blood vessels continued to stain positive (Fig. 4J). However, staining was no longer evident in muscle (Fig. 4K). Positively staining cells with fibroblast and monocytic morphology continued to be present in the dermis (Fig. 4L), and the latter were occasionally present in blood vessels (Fig. 4M). Cells with macrophage and fibroblast morphology were also occasionally present in connective tissue (data not shown). No staining was seen in the epidermis (Fig. 4N). In IRF3/7$^{-/-}$ mice, cells lining blood vessels (Fig. 4O), muscle cells (Fig. 4P), dermal cells with fibroblast morphology (Fig. 4Q), and cells in

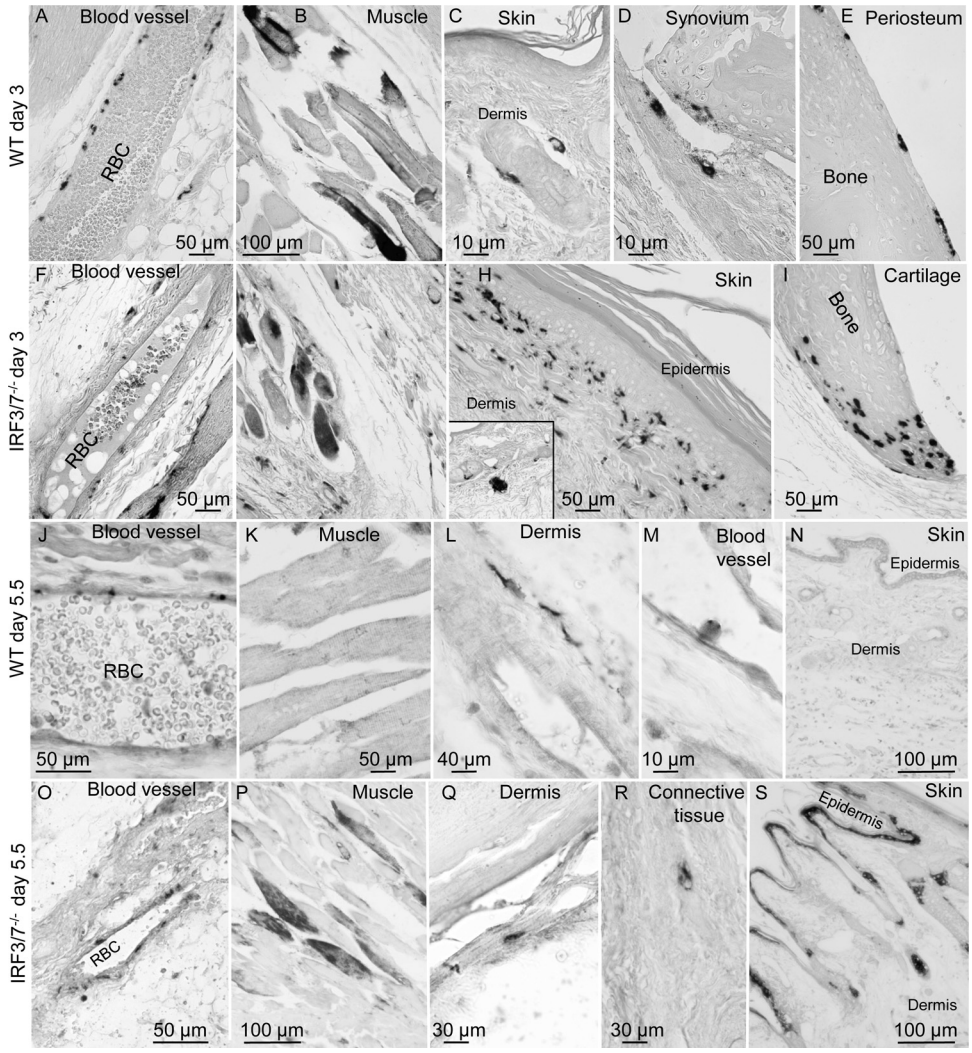

FIG 4 Detection of CHIKV RNA by *in situ* hybridization. CHIKV RNA was detected by *in situ* hybridization in tissues from CHIKV-infected (i) WT mice 3 days postinfection (A to E), (ii) IRF3/7$^{-/-}$ mice 3 days postinfection (F to I), (iii) WT mice 5.5 days postinfection (J to N), and (iv) IRF3/7$^{-/-}$ mice 5.5 days postinfection (O to S). Staining is shown for cells lining blood vessel walls (A, F, J, and O) (RBC, red blood cells), skeletal muscle (B, G, K, and P), skin (C, H, N, and S), synovial membrane (D), periosteum (E), articular cartilage (I), dermis (L and Q), a cell within a blood vessel (M), and connective tissue (R). Enlarged images of selected cells with more detailed descriptions are shown in File S6 in the supplemental material.

connective tissue with monocytic morphology (Fig. 4R) continued to be stained. The epidermis also stained positive in IRF3/7$^{-/-}$ mice in several areas (Fig. 4S), suggesting infection of keratinocytes. No such staining was observed in WT mice (data not shown).

No staining was obtained using (i) tissue from uninfected mice, (ii) antisense probes coding for the same region of Ross River virus (RRV), or (iii) CHIKV sense probes (data not shown). Minus-strand RNA, which would be detected by sense probes, is substantially more short-lived and less abundant than positive-strand RNA in alphavirus infections.

The pattern and the type of cells infected in IRF3/7$^{-/-}$ mice thus appeared to be distinct from those infected in WT mice. In IRF3/7$^{-/-}$ mice, articular cartilage cells and more dermal fibroblasts appeared to be infected by day 3, and on day 5.5 there was ongoing skeletal muscle infection and infection of epidermis. Although hemorrhage was readily detected in IRF3/7$^{-/-}$ (but not in WT) mice, infection of blood vessel lining cells did not appear to be any more extensive in IRF3/7$^{-/-}$ than in WT mice (compare Fig. 4A with Fig. 4F and Fig. 4J with Fig. 4O; also data not shown).

Clinical signs in CHIKV-infected IRF3/7$^{-/-}$ mice were consistent with hemorrhagic shock. On day 2 after infection of IRF3/7$^{-/-}$ mice, a significant fever concomitant with the peak viremia was observed (a concomitance also seen in CHIKV patients [57]), with a dramatic drop in body temperature seen on days 3 and 4 (Fig. 5A). Hypothermia is indicative of hypovolemic shock, and a sudden change from fever to hypothermia is also a predictor of impending dengue shock syndrome (DSS) (44). WT mice infected with CHIKV did not develop a detectable fever, nor did they show a significant drop in body temperature on day 4 or 5 postinfection, although a slight dip was evident on day 3 (Fig. 5A).

The urine output of IRF3/7$^{-/-}$ mice 4 to 5 days postinfection was dramatically reduced (oliguria) compared with that of WT

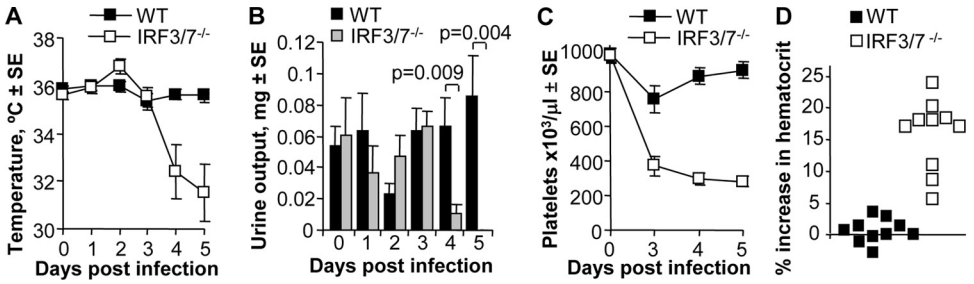

FIG 5 Clinical observations. (A) Body temperatures measured by a thermocouple placed in the pit of the hind leg ($n = 4$ to 16 per group). IRF3/7$^{-/-}$ mice showed a significant fever on day 2 ($P = 0.004$ for day 0 versus day 2). Temperatures were also higher in IRF3/7$^{-/-}$ mice than WT mice on day 2 ($P = 0.01$). Temperatures were significantly lower in IRF3/7$^{-/-}$ mice than WT mice on days 4 and 5 ($P < 0.001$). (B) Scruff-induced urine output. Differences were significant on days 4 and 5 ($n = 8$ to 10 per group). (C) Platelet count. Platelet counts were significantly lower in IRF7$^{-/-}$ than WT mice on days 3, 4, and 5 postinfection ($P = 0.001$, $P < 0.001$, and $P < 0.001$, respectively; *t* test; $n = 8$ to 10 per group). (D) Percentage increase in hematocrit in WT and IRF3/7$^{-/-}$ mice on day 5 postinfection compared with control uninfected mice ($P < 0.001$; $n = 10$ or 11 per group). All statistics were obtained by the Mann-Whitney U test. The data were obtained from two to four independent experiments.

mice (Fig. 5B). This is also a feature of hypovolemic shock (67) and is observed in DSS (61).

A marked thrombocytopenia was observed in IRF3/7$^{-/-}$ mice on days 4 to 5 postinfection, with mice showing a mean ~70% drop in platelet counts to $<300 \times 10^3$/μl (Fig. 5C). In humans, the normal range for platelet counts is 150×10^3 to 400×10^3/μl, which is much lower than the ~$1{,}000 \times 10^3$/μl seen in C57BL/6 mice (Fig. 5C). In humans, a 70% drop would result in platelet counts of 45×10^3 to 120×10^3/μl. Thrombocytopenia with platelet counts of $<100 \times 10^3$/μl is one of the current criteria for the diagnosis of dengue hemorrhagic fever/dengue shock syndrome (DHF/DSS) (56).

Measurement of the hematocrit in IRF3/7$^{-/-}$ mice showed a mean 15.8% (range, 7 to 24%) increase on day 5 postinfection (Fig. 5D), whereas infected WT mice showed no significant change from uninfected controls (Fig. 5D). Elevated hematocrits are indicative of hemoconcentration and plasma leakage. Hematocrit increases of >20% are a diagnostic criterion for DHF/DSS (61).

The clinical features preceding mortality in CHIKV-infected IRF3/7$^{-/-}$ mice, taken together with the histology (which showed widespread edema), strongly suggest that death in these animals was due to hypovolemic shock.

IFN-α/β receptor-deficient (IFNAR$^{-/-}$) mice. CHIKV infection of IFNAR$^{-/-}$ mice gave results similar to those obtained with IRF3/7$^{-/-}$ mice (see File S3 in the supplemental material), suggesting that loss of IFN-α/β (rather than other IRF3/7-dependent) responses predisposes animals to hemorrhagic shock.

IRF3/7$^{-/-}$ mice could be protected by vaccination. Vaccination with inactivated CHIKV fully protected IRF3/7$^{-/-}$ mice against viremia and disease, suggesting that mortality of IRF3/7$^{-/-}$ mice after CHIKV infection was not due to a defect in antibody responses (see File S4 in the supplemental material).

Prophylactic IFN-α treatment of IRF3/7$^{-/-}$ mice failed to prevent mortality. IFN-α at 10^3 IU (intravenously [i.v.]) significantly reduced the viremia and prevented disease in adult WT mice if given before CHIKV challenge (15). Injection (i.v.) of a 10-fold-higher dose (10^4 IU) into IRF3/7$^{-/-}$ mice prior to infection was only able to delay mortality by 24 to 48 h; although this was significant, all mice ultimately died (Fig. 6A). Foot swelling was also delayed by ~24 h but not prevented (data not shown).

Adoptive transfer of WT splenocytes or WT splenic CD11b$^+$ cells into IRF3/7$^{-/-}$ mice delayed but was unable to prevent mortality (data not shown), consistent with the observation that hematopoietic cells do not produce sufficient IFN-α/β to protect mice against CHIKV infection (51).

IFN-α treatment did not effectively inhibit CHIKV replication in IRF3/7$^{-/-}$ MEFs. The inability of prophylactic IFN-α treatment to prevent CHIKV-mediated mortality in IRF3/7$^{-/-}$ mice (Fig. 6A) is perhaps surprising. We thus investigated the ability of IFN-α to reduce CHIKV replication in IRF3/7$^{-/-}$ cells *in vitro*, by treating MEFs from IRF3/7$^{-/-}$ mice with a range of

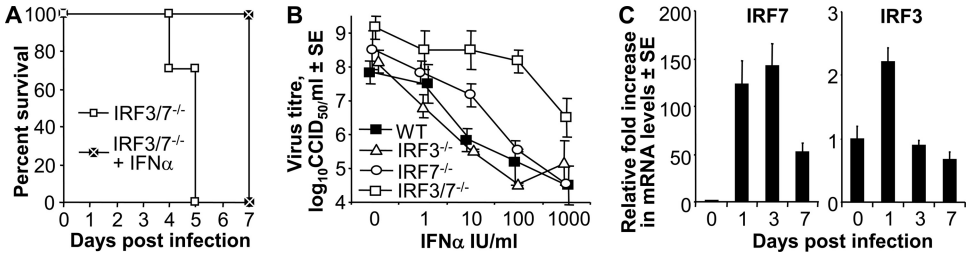

FIG 6 IFN-α treatment and IRF7 induction. (A) IRF3/7$^{-/-}$ mice ($n = 3$) were treated with 10^4 IU of IFN-α i.v. 1 day before infection with CHIKV, and survival was monitored over time (IRF3/7$^{-/-}$ + IFN-α) and compared with that infected IRF3/7$^{-/-}$ mice not receiving IFN-α ($n = 24$) (log rank test, $P = 0.001$). (B) MEFs from IRF3/7$^{-/-}$, IRF3$^{-/-}$, IRF7$^{-/-}$, and WT mice were treated *in vitro* with the indicated concentration of IFN-α overnight prior to CHIKV infection (MOI = 0.1). After washing, the cells were cultured for 24 h, and the supernatants were then assayed for viral titers ($n = 3$). (C) Quantitative real-time RT-PCR of IRF3 and IRF7 mRNA expression in CHIKV-infected feet normalized to RPL13A ($n = 6$). Levels are expressed relative to those on day 0.

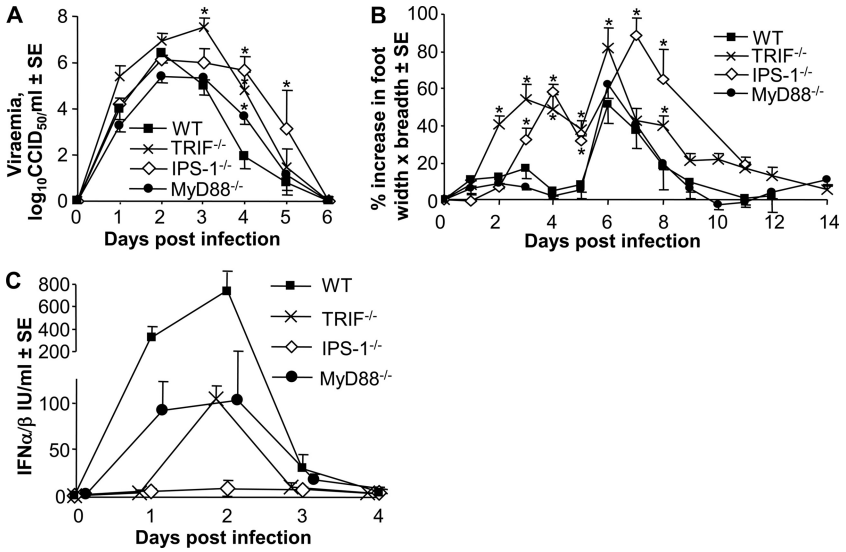

FIG 7 CHIKV infection of IPS-1$^{-/-}$, MyD88$^{-/-}$ and TRIF$^{-/-}$ mice. Viremia, foot swelling, and serum IFN-α/β levels following CHIKV infection of WT, TRIF$^{-/-}$, IPS-1$^{-/-}$, and MyD88$^{-/-}$ mice (8 to 12 weeks old). (A) Viremia. Significant differences between the knockout and WT mice are indicated (*). TRIF$^{-/-}$ mice ($n = 11$) showed higher viremias on days 3 and 4 than WT mice ($n = 21$ to 25; $P = 0.001$ and 0.004, respectively). IPS-1$^{-/-}$ mice ($n = 3$) showed higher viremias on days 4 and 5 than WT mice ($P = 0.029$ and 0.048, respectively). MyD88$^{-/-}$ ($n = 8$) mice showed a higher viremia on day 4 ($P = 0.013$). (B) Foot swelling. TRIF$^{-/-}$ feet ($n = 10$ to 32) were significantly larger on days 2 to 6 and 8, and IPS-1$^{-/-}$ feet ($n = 6$) were significantly larger on days 3 to 5, 7, and 8 than WT feet ($n = 14$ to 28; $P < 0.006$ for all comparisons). Significant differences are indicated (*) ($n = 8$ to 22 for MyD88$^{-/-}$ feet). (C) Serum IFN-α/β levels as determined by bioassay (WT, $n = 7$ to 11; IPS-1$^{-/-}$, $n = 3$; MyD88$^{-/-}$, $n = 5$; and TRIF$^{-/-}$, $n = 5$). On day 1, IFN-α/β levels were significantly higher in MyD88$^{-/-}$ mice than in TRIF$^{-/-}$ and IPS-1$^{-/-}$ mice ($P = 0.009$ and 0.025, respectively). (IFN-α/β levels in IPS$^{-/-}$ mice peaked on day 2 at 8.7 ± 1.5 IU/ml.) On day 2, levels in WT mice were significantly higher than those in MyD88$^{-/-}$ and TRIF$^{-/-}$ mice ($P = 0.004$ and 0.002, respectively). (All statistics were obtained by the Mann-Whitney U test.)

IFN-α concentrations. The cells were then infected with CHIKV, and virus production was measured. WT MEFs produced significantly lower titers of CHIKV after treatment with IFN-α concentrations of ≥10 IU/ml (Fig. 6B) (*t* test, $P < 0.006$). In contrast, there was no significant effect on CHIKV titers in IRF3/7$^{-/-}$ MEFs until 1,000 IU/ml of IFN-α was used (Fig. 6B) (*t* test, $P = 0.028$). IRF7$^{-/-}$ MEFs showed an intermediate phenotype requiring treatment with 100 IU/ml IFN-α before significant reductions in CHIKV titers were seen (Fig. 6B) (Mann-Whitney U test, $P = 0.037$). CHIKV titers in IRF3$^{-/-}$ MEFs were not significantly different from those in WT MEFs. IRF3/7$^{-/-}$ MEFs thus needed to be treated with 100× more and IRF7$^{-/-}$ MEFs with 10× more IFN-α before significant reductions in CHIKV titers were achieved.

IRF7 mRNA was upregulated >100-fold in WT mice after CHIKV infection. Upregulation of IRF7 (but not IRF3) is important for the positive feedback and induction of IFN-αs that generate a robust IFN-α/β response following viral infection in MEFs (33, 48, 49). The likely importance of IRF7 for optimal IFN-α/β production after CHIKV infection was also suggested by the low level of serum IFN-α/β production in IRF7$^{-/-}$ mice after CHIKV infection (Fig. 2A). Quantitative RT-PCR analysis of feet from CHIKV-infected WT mice illustrated that IRF7 mRNA, but not IRF3 mRNA, was upregulated >100-fold after CHIKV infection (Fig. 6C). (IFN-α treatment also upregulated IRF7 mRNA expression in MEFs [data not shown].) Upregulation of IRF7 in nonhematopoietic cells (51) following CHIKV infection thus likely promotes IFN-α/β production and protection against exacerbated disease. These data also suggest that an important activity of prophylactic IFN-α treatment against CHIKV in WT mice is upregulation of IRF7, rather than the induction of an antiviral state.

Roles of TRIF, IPS-1, and MyD88. IRF3 and IRF7 lie downstream of RIG-I/Mda5/IPS-1, TLR3/TRIF, and TLR7/MyD88 pathways, and although signaling via these pathways during CHIKV infections has been reported (51, 53, 66), the relative importance of these pathways for controlling infection, preventing disease, and inducing IFN-α/β *in vivo* has not been investigated.

CHIKV infection of TRIF$^{-/-}$, IPS-1$^{-/-}$, and MyD88$^{-/-}$ mice resulted in significantly higher mean viremias on days 3 and 4, days 4 and 5, and day 4 postinfection, respectively, than that of WT mice (Fig. 7A). Foot swelling was significantly more pronounced in TRIF$^{-/-}$ and IPS-1$^{-/-}$ mice, beginning earlier, peaking higher, and lasting longer (particularly in IPS$^{-/-}$ mice) than in WT mice (Fig. 7B). There was no significant difference in foot swelling in MyD88$^{-/-}$ mice. For serum IFN-α/β levels, the ranking was WT > MyD88$^{-/-}$ > TRIF$^{-/-}$ > IPS-1$^{-/-}$ mice, which generally follows the viremia and foot swelling data (when area under the curves is considered). These data suggest that RIG-I/Mda5 signaling via IPS-1 is the most important for IFN-α/β production in response to CHIKV infection, followed by the TLR3/TRIF$^{-/-}$ pathway, with the MyD88$^{-/-}$-dependent pathway being the least important.

DISCUSSION

Here we show that IRF3 and IRF7 are critical for survival after CHIKV infection, consistent with recent studies (50). CHIKV infection of IRF3/7$^{-/-}$ mice resulted in no detectable serum IFN-α/β, large increases in virus titers, and high levels of serum IFN-γ, TNF, IL-6, and MCP-1, with animals ultimately dying of hemorrhagic shock. Mortality did not appear to be due to defective antibody responses, as vaccination fully protected IRF3/7$^{-/-}$ mice. Prophylactic IFN-α treatment had only limited effect against

CHIKV infection both *in vivo* (in IRF3/7$^{-/-}$ mice) and *in vitro* (in IRF3/7$^{-/-}$ MEFs), with upregulation of IRF7 likely being required for optimal IFN-α/β production (33, 48, 49). Our studies suggest that CHIKV infection leads to IFN-α/β production primarily via the RIG-I/Mda5/IPS-1 and TLR3/TRIF$^{-/-}$ pathways, with downstream signaling involving IRF7 (and to a lesser extent IRF3).

The disease manifestations in CHIKV-infected IRF3/7$^{-/-}$ mice included fever and edema, features that are often observed with human CHIKV disease (57). A skin rash is also common in CHIKV disease patients (57); whether this is due to infection of keratinocytes is unclear (41), as the present study was able to detect epidermal infection only in IRF3/7$^{-/-}$ and not WT mice. Herein we also provide the first evidence that CHIKV can infect mature skeletal muscle cells. So far, only CHIKV infection of human muscle satellite cells has been reported (40), although RRV has been shown to infect skeletal muscle in young mice (34). Myocyte infection may in part explain the myalgia, a common manifestation of human CHIKV disease (57). Infection of chondrocytes by CHIKV has not previously been reported, although infection of the periosteum by Sindbis virus (18) and RRV in young mice (34) has been observed; such infections are likely to contribute to rheumatic disease. CHIKV infection of monocytes/macrophages, fibroblasts, and endothelial cells *in vivo* has been reported previously (19, 27). The more severe manifestations seen in IRF3/7$^{-/-}$ (and IFNAR$^{-/-}$) mice, hemorrhage, thrombocytopenia, and hypovolemic shock, have also been reported for severe CHIKV infections in human neonates and children (16, 47), with such manifestations occasionally associated with mortality in neonates (16, 37, 45, 47, 57). Human neonates have defective innate antiviral responses, including defective IRF7-mediated responses (12, 31). Hemorrhagic fever associated with CHIKV infections in children (13, 24, 45) and some adults (39, 47) has also been reported. CHIKV infection of IRF3/7$^{-/-}$ (and IFNAR$^{-/-}$) mice thus recapitulates many of the features seen during severe human disease. These findings thus suggest that a paucity of IFN-α/β responses may predispose human hosts to severe CHIKV disease.

The parallels between the pathological and clinical signs preceding mortality in CHIKV-infected IRF3/7$^{-/-}$ and IFNAR$^{-/-}$ mice and those seen in humans with DHF/DSS are striking. Oliguria, increased hematocrit, fever followed by hypothermia, edema, hemorrhage, and thrombocytopenia are all features of DHF/DSS. Elevated levels of IFN-γ, TNF, IL-6, and MCP-1 (CCL2) are also key players in DHF/DSS (30, 42). As IRF3/7$^{-/-}$ and IFNAR$^{-/-}$ mice lack IFN-α/β responses, an important driver of DHF/DSS may also be inadequate IFN-α/β responses. This concept was proposed previously based on the ability of antibody-dependent enhancement to suppress IFN-α/β responses (17, 58). The idea is also supported by an array analysis of DSS patients, which showed that type 1 IFN-induced gene transcripts were less abundant in DSS patients (54). In addition, IRF7 has also been identified as a key transcription factor mediating the early response to dengue (20). (Conceivably, inhibition of IFN-α/β receptor signaling by dengue virus [36] is also involved, with CHIKV being reported to have similar activity [14].)

The very high levels of proinflammatory mediators, particularly IFN-γ and TNF, seen in CHIKV-infected IRF3/7$^{-/-}$ and IFNAR$^{-/-}$ mice are likely important contributors to vascular leakage and shock (42). However, the paucity of IFN-α/β responses, rather than the elevated viral load, may be the main factor responsible for the high levels of these cytokines. IFN-α/β has been shown to inhibit IFN-γ production by NK and T cells (7, 38), and in mice with high *Trypanosome cruzi* burdens, IFN-α/β has also been shown to suppress IFN-γ production (6). IFN-α/β can also suppress the responses to IFN-γ by downregulating the IFN-γ receptor (43). The increase in IFN-γ levels in CHIKV-infected IRF3/7$^{-/-}$ and IFNAR$^{-/-}$ mice is probably responsible for increased TNF production by macrophages (43). These observations support the view that IFN-α/β plays a critical role in suppressing excessive IFN-γ-mediated immune pathology during acute infection.

For both dengue virus and CHIKV infections, it remains unclear which cells are producing and responding to protective IFN-α/β *in vivo*. Dengue virus can infect monocytes/macrophages (17), fibroblasts (26), endothelial cells (11), skeletal muscle cells (46), and keratinocytes (59). Herein we provide evidence that all these cell types are also infected by CHIKV *in vivo*. Although hematopoietic cells (e.g., plasmacytoid dendritic cells) are often believed to be the main producers of IFN-α/β *in vivo*, hematopoietic cells do not appear to be involved in production of protective IFN-α/β during CHIKV infection (51). The importance of IPS-1 for IFN-α/β production supports the view that nonhematopoietic cells (51) directly infected by CHIKV are an important source of protective IFN-α/β *in vivo*. Although detection of viral double-stranded RNA from alphavirus-infected cells by hematopoietic cell TLR3 is well established (10, 52), TLR3 is also expressed and/or can be upregulated on endothelial cells (70), dermal fibroblasts (1), and keratinocytes (69). All these cell types also express and/or can upregulate IRF7 and produce IFN-α/β (3, 33, 48, 63). Detection of alphaviral single-stranded RNA by TLR7 has not yet been formally demonstrated but might be assumed, given its role in infection with other single-stranded RNA viruses (62). However, the minor phenotypes seen in MyD88$^{-/-}$ mice suggest that the TLR7/MyD88$^{-/-}$ pathway plays a relatively less important role during CHIKV infection and disease.

The importance of IPS-1 in nonhematopoietic cells for protective responses to CHIKV infection was recently reported (50) and is consistent with the findings presented herein. MyD88 was previously reported to be important for preventing CHIKV dissemination, with 0.5- to 1-log-higher viremia (on day 2) and tissue viral titers (on day 3) observed in MyD88$^{-/-}$ mice compared with WT mice (51). We did not analyze tissue titers in MyD88$^{-/-}$ mice but saw a ~1.7-log-higher serum viremia in MyD88$^{-/-}$ mice than in WT mice on day 4. The results are thus broadly comparable, with differences likely being attributable to differences in the infection models (e.g., virus preparation, detection method, and route of inoculation).

A striking feature of CHIKV infection in IRF3/7$^{-/-}$ mice is the paucity of infiltrating cells compared with levels in IRF3$^{-/-}$, IRF7$^{-/-}$, and WT mice. Infiltrates in WT mice primarily contain monocytes and macrophages (15), with infiltration of these cells being largely dependent on chemokine (C-C motif) receptor 2 (CCR2), the receptor for MCP-1/CCL2 (Suan Poo, unpublished data). Despite the paucity of IFN-α/β (8), MCP-1 was very efficiently produced in CHIKV-infected IRF3/7$^{-/-}$ mice, illustrating that loss of MCP-1 was not responsible. Two factors may explain the lack of infiltrating cells in CHIKV-infected IRF3/7$^{-/-}$ mice. First, IFN-α/β appears to be required for differentiation of resting Ly6C^{lo} monocytes into inflammatory Ly6C^{hi} monocytes, with only the latter being able to migrate in response to MCP-1/CCR2 (29). Second, high levels of IFN-γ and TNF have been shown to

downregulate expression of CCR2 in monocytes (60, 65), and TNF has also been shown to downregulate CCR2 expression in dendritic cells (64).

In summary, the studies described herein highlight the critical role of IRF7 (and to a lesser extent IRF3) in the production of protective IFN-α/β via IPS-1- and TRIF-dependent (and to lesser extent MyD88-dependent) pathways. The studies also illustrate the importance of IFN-α/β responses in protection against virus-induced hemorrhage and shock, with a compromised IFN-α/β response being associated with high levels of IFN-γ and TNF. By analogy, this work suggests that a paucity of IFN-α/β may also play an important role in DHF/DSS.

ACKNOWLEDGMENTS

We thank Clay Winterford (Histotechnology Facility) and animal house staff (QIMR) for excellent support and M. S. Diamond for supplying knockout mice.

This work was funded by the NHMRC, Australia. Equipment was funded by the Queensland Tropical Health Alliance and a donation from Ed Westaway, Royal Australian Air Force Association. A.S. and A.A.K. are research fellows with the NHMRC, and P.A.R. is a postdoctoral fellow with the Canadian Institutes of Health Research.

The funders had no role in study design, data collection and analysis, decision to publish, or preparation of the manuscript.

REFERENCES

1. **Agarwal SK, et al.** 2011. Toll-like receptor 3 upregulation by type I interferon in healthy and scleroderma dermal fibroblasts. Arthritis Res. Ther. **13**:R3. doi:10.1186/ar3221.
2. **Ali U, Isahak I, Rahman MM.** 2011. Chikungunya confused with dengue In Malaysia: clinical, serological and molecular perspective. Internet J. Microbiol. **9**(2). doi:10.5580/647.
3. **Buss C, et al.** 2010. Essential role of mitochondrial antiviral signaling, IFN-regulatory factor (IRF)3, and IRF7 in Chlamydophila pneumoniae-mediated IFN-beta response and control of bacterial replication in human endothelial cells. J. Immunol. **184**:3072–3078.
4. **Chattopadhyay S, Yamashita M, Zhang Y, Sen GC.** 2011. The IRF-3/Bax-mediated apoptotic pathway, activated by viral cytoplasmic RNA and DNA, inhibits virus replication. J. Virol. **85**:3708–3716.
5. **Chen LH, Wilson ME.** 2010. Dengue and chikungunya infections in travelers. Curr. Opin. Infect. Dis. **23**:438–444.
6. **Chessler AD, Caradonna KL, Da'dara A, Burleigh BA.** 2011. Type I interferons increase host susceptibility to Trypanosoma cruzi infection. Infect. Immun. **79**:2112–2119.
7. **Cousens LP, Orange JS, Su HC, Biron CA.** 1997. Interferon-alpha/beta inhibition of interleukin 12 and interferon-gamma production in vitro and endogenously during viral infection. Proc. Natl. Acad. Sci. U. S. A. **94**:634–639.
8. **Crane MJ, Hokeness-Antonelli KL, Salazar-Mather TP.** 2009. Regulation of inflammatory monocyte/macrophage recruitment from the bone marrow during murine cytomegalovirus infection: role for type I interferons in localized induction of CCR2 ligands. J. Immunol. **183**:2810–2817.
9. **Daffis S, et al.** 2011. The naturally attenuated Kunjin strain of West Nile virus shows enhanced sensitivity to the host type I interferon response. J. Virol. **85**:5664–5668.
10. **Daffis S, Suthar MS, Szretter KJ, Gale M, Jr, Diamond MS.** 2009. Induction of IFN-beta and the innate antiviral response in myeloid cells occurs through an IPS-1-dependent signal that does not require IRF-3 and IRF-7. PLoS Pathog. **5**:e1000607. doi:10.1371/journal.ppat.1000607.
11. **Dalrymple N, Mackow ER.** 2011. Productive dengue virus infection of human endothelial cells is directed by heparan sulfate-containing proteoglycan receptors. J. Virol. **85**:9478–9485.
12. **Danis B, et al.** 2008. Interferon regulatory factor 7-mediated responses are defective in cord blood plasmacytoid dendritic cells. Eur. J. Immunol. **38**:507–517.
13. **Deller JJ, Jr, Russell PK.** 1968. Chikungunya disease. Am. J. Trop. Med. Hyg. **17**:107–111.
14. **Fros JJ, et al.** 2010. Chikungunya virus nonstructural protein 2 inhibits type I/II interferon-stimulated JAK-STAT signaling. J. Virol. **84**:10877–10887.
15. **Gardner J, et al.** 2010. Chikungunya virus arthritis in adult wild-type mice. J. Virol. **84**:8021–8032.
16. **Gerardin P, et al.** 2008. Multidisciplinary prospective study of mother-to-child chikungunya virus infections on the island of La Reunion. PLoS Med. **5**:e60. doi:10.1371/journal.pmed.0050060.
17. **Halstead SB, Mahalingam S, Marovich MA, Ubol S, Mosser DM.** 2010. Intrinsic antibody-dependent enhancement of microbial infection in macrophages: disease regulation by immune complexes. Lancet Infect. Dis. **10**:712–722.
18. **Heise MT, Simpson DA, Johnston RE.** 2000. Sindbis-group alphavirus replication in periosteum and endosteum of long bones in adult mice. J. Virol. **74**:9294–9299.
19. **Her Z, et al.** 2010. Active infection of human blood monocytes by Chikungunya virus triggers an innate immune response. J. Immunol. **184**:5903–5913.
20. **Hoang LT, et al.** 2010. The early whole-blood transcriptional signature of dengue virus and features associated with progression to dengue shock syndrome in Vietnamese children and young adults. J. Virol. **84**:12982–12994.
21. **Hoarau JJ, et al.** 2010. Persistent chronic inflammation and infection by Chikungunya arthritogenic alphavirus in spite of a robust host immune response. J. Immunol. **184**:5914–5927.
22. **Honda K, et al.** 2005. IRF-7 is the master regulator of type-I interferon-dependent immune responses. Nature **434**:772–777.
23. **Johnson BJ, et al.** 2005. Heat shock protein 10 inhibits lipopolysaccharide-induced inflammatory mediator production. J. Biol. Chem. **280**:4037–4047.
24. **Khai Ming C, et al.** 1974. Clinical and laboratory studies on haemorrhagic fever in Burma, 1970–72. Bull. World Health Organ. **51**:227–235.
25. **Kumar H, et al.** 2006. Essential role of IPS-1 in innate immune responses against RNA viruses. J. Exp. Med. **203**:1795–1803.
26. **Kurane I, Janus J, Ennis FA.** 1992. Dengue virus infection of human skin fibroblasts in vitro production of IFN-beta, IL-6 and GM-CSF. Arch. Virol. **124**:21–30.
27. **Labadie K, et al.** 2010. Chikungunya disease in nonhuman primates involves long-term viral persistence in macrophages. J. Clin. Invest. **120**:894–906.
28. **La Linn M, Bellett AJ, Parsons PG, Suhrbier A.** 1995. Complete removal of mycoplasma from viral preparations using solvent extraction. J. Virol. Methods **52**:51–54.
29. **Lee PY, et al.** 2009. Type I interferon modulates monocyte recruitment and maturation in chronic inflammation. Am. J. Pathol. **175**:2023–2033.
30. **Lee YR, et al.** 2006. MCP-1, a highly expressed chemokine in dengue haemorrhagic fever/dengue shock syndrome patients, may cause permeability change, possibly through reduced tight junctions of vascular endothelium cells. J. Gen. Virol. **87**:3623–3630.
31. **Levy O.** 2007. Innate immunity of the newborn: basic mechanisms and clinical correlates. Nat. Rev. Immunol. **7**:379–390.
32. **Lidbury BA, Simeonovic C, Maxwell GE, Marshall ID, Hapel AJ.** 2000. Macrophage-induced muscle pathology results in morbidity and mortality for Ross River virus-infected mice. J. Infect. Dis. **181**:27–34.
33. **Marie I, Durbin JE, Levy DE.** 1998. Differential viral induction of distinct interferon-alpha genes by positive feedback through interferon regulatory factor-7. EMBO J. **17**:6660–6669.
34. **Morrison TE, et al.** 2006. Characterization of Ross River virus tropism and virus-induced inflammation in a mouse model of viral arthritis and myositis. J. Virol. **80**:737–749.
35. **Munoz A, Carrasco L.** 1984. Action of human lymphoblastoid interferon on HeLa cells infected with RNA-containing animal viruses. J. Gen. Virol. **65**:377–390.
36. **Munoz-Jordan JL.** 2010. Subversion of interferon by dengue virus. Curr. Top. Microbiol. Immunol. **338**:35–44.
37. **Nair PM.** 2008. Correspondence; Chikungunya in neonates. Indian Pediatr. **45**:605.
38. **Nguyen KB, et al.** 2002. Coordinated and distinct roles for IFN-alpha beta, IL-12, and IL-15 regulation of NK cell responses to viral infection. J. Immunol. **169**:4279–4287.
39. **Nimmannitya S, Halstead SB, Cohen SN, Margiotta MR.** 1969. Dengue and chikungunya virus infection in man in Thailand, 1962-1964. I. Observations on hospitalized patients with hemorrhagic fever. Am. J. Trop. Med. Hyg. **18**:954–971.

40. **Ozden S, et al.** 2007. Human muscle satellite cells as targets of Chikungunya virus infection. PLoS One **2**:e527. doi:10.1371/journal.pone.0000527.
41. **Pakran J, et al.** 2011. Purpuric macules with vesiculobullous lesions: a novel manifestation of Chikungunya. Int. J. Dermatol. **50**:61–69.
42. **Pang T, Cardosa MJ, Guzman MG.** 2007. Of cascades and perfect storms: the immunopathogenesis of dengue haemorrhagic fever-dengue shock syndrome (DHF/DSS). Immunol. Cell Biol. **85**:43–45.
43. **Rayamajhi M, Humann J, Penheiter K, Andreasen K, Lenz LL.** 2010. Induction of IFN-alphabeta enables Listeria monocytogenes to suppress macrophage activation by IFN-gamma. J. Exp. Med. **207**:327–337.
44. **Rigau-Perez JG, Laufer MK.** 2006. Dengue-related deaths in Puerto Rico, 1992-1996: diagnosis and clinical alarm signals. Clin. Infect. Dis. **42**:1241–1246.
45. **Robin S, et al.** 2008. Neurologic manifestations of pediatric chikungunya infection. J. Child Neurol. **23**:1028–1035.
46. **Salgado DM, et al.** 2010. Heart and skeletal muscle are targets of dengue virus infection. Pediatr. Infect. Dis. J. **29**:238–242.
47. **Sarkar JK, Chatterjee SN, Chakravarti SK, Mitra AC.** 1965. Chikungunya virus infection with haemorrhagic manifestations. Indian J. Med. Res. **53**:921–925.
48. **Sato M, et al.** 1998. Positive feedback regulation of type I IFN- genes by the IFN-inducible transcription factor IRF-7. FEBS Lett. **441**:106–110.
49. **Sato M, et al.** 2000. Distinct and essential roles of transcription factors IRF-3 and IRF-7 in response to viruses for IFN-alpha/beta gene induction. Immunity **13**:539–548.
50. **Schilte C, et al.** 2012. Cutting edge: independent roles for IRF-3 and IRF-7 in hematopoietic and nonhematopoietic cells during host response to Chikungunya infection. J. Immunol. **188**:2967–2971.
51. **Schilte C, et al.** 2010. Type I IFN controls chikungunya virus via its action on nonhematopoietic cells. J. Exp. Med. **207**:429–442.
52. **Schulz O, et al.** 2005. Toll-like receptor 3 promotes cross-priming to virus-infected cells. Nature **433**:887–892.
53. **Schwartz O, Albert ML.** 2010. Biology and pathogenesis of chikungunya virus. Nat. Rev. Microbiol. **8**:491–500.
54. **Simmons CP, et al.** 2007. Patterns of host genome-wide gene transcript abundance in the peripheral blood of patients with acute dengue hemorrhagic fever. J. Infect. Dis. **195**:1097–1107.
55. **Sourisseau M, et al.** 2007. Characterization of reemerging chikungunya virus. PLoS Pathog. **3**:e89. doi:10.1371/journal.ppat.0030089.
56. **Srikiatkhachorn A, Green S.** 2010. Markers of dengue disease severity. Curr. Top. Microbiol. Immunol. **338**:67–82.
57. **Suhrbier A, Jaffar-Bandjee MC, Gasque P.** 2012. Arthritogenic alphaviruses–an overview. Nat. Rev. Rheumatol. **8**:420–429.
58. **Suhrbier A, La Linn M.** 2003. Suppression of antiviral responses by antibody-dependent enhancement of macrophage infection. Trends Immunol. **24**:165–168.
59. **Surasombatpattana P, et al.** 2011. Dengue virus replication in infected human keratinocytes leads to activation of antiviral innate immune responses. Infect. Genet. Evol. **11**:1664–1673.
60. **Tangirala RK, Murao K, Quehenberger O.** 1997. Regulation of expression of the human monocyte chemotactic protein-1 receptor (hCCR2) by cytokines. J. Biol. Chem. **272**:8050–8056.
61. **Teik OC.** 2001. A guide to DHF/DSS management—the Singapore experience. Dengue Bull. **25**:45–49.
62. **Town T, et al.** 2009. Toll-like receptor 7 mitigates lethal West Nile encephalitis via interleukin 23-dependent immune cell infiltration and homing. Immunity **30**:242–253.
63. **van der Fits L, van der Wel LI, Laman JD, Prens EP, Verschuren MC.** 2004. In psoriasis lesional skin the type I interferon signaling pathway is activated, whereas interferon-alpha sensitivity is unaltered. J. Investig. Dermatol. **122**:51–60.
64. **Vecchi A, et al.** 1999. Differential responsiveness to constitutive vs. inducible chemokines of immature and mature mouse dendritic cells. J. Leukoc. Biol. **66**:489–494.
65. **Weber C, et al.** 1999. Downregulation by tumor necrosis factor-alpha of monocyte CCR2 expression and monocyte chemotactic protein-1-induced transendothelial migration is antagonized by oxidized low-density lipoprotein: a potential mechanism of monocyte retention in atherosclerotic lesions. Atherosclerosis **145**:115–123.
66. **White LK, et al.** 2011. Chikungunya virus induces IPS-1-dependent innate immune activation and protein kinase R-independent translational shutoff. J. Virol. **85**:606–620.
67. **Worthley LI.** 2000. Shock: a review of pathophysiology and management. Part II. Crit. Care Resusc. **2**:66–84.
68. **Yamamoto M, et al.** 2003. Role of adaptor TRIF in the MyD88-independent toll-like receptor signaling pathway. Science **301**:640–643.
69. **Zhang SQ, et al.** 2011. Interleukin 29 enhances expression of toll receptor 3 and mediates antiviral signals in human keratinocytes. Inflamm. Res. **60**:1031–1037.
70. **Zimmer S, et al.** 2011. Activation of endothelial toll-like receptor 3 impairs endothelial function. Circ. Res. **108**:1358–1366.